Application value of multimodal ultrasound in differential diagnosis of thyroid nodules

J. Zhai* and J. Li

Head and Neck Cancer Surgery, Tangshan people's Hospital, Tangshan City, Hebei Province, China

ABSTRACT

► *Original article*

Background: Background: While conventional ultrasound (US) remains the first-line diagnostic tool, its limitations in distinguishing benign from malignant nodules necessitate exploring complementary techniques. This study aimed to evaluate the potential of integrating contrast-enhanced ultrasound (CEUS) and ultrasound elastography (UE) alongside conventional US to improve diagnostic accuracy compared to individual modalities. ***Materials and Methods:*** This retrospective analysis was conducted at Tangshan people's Hospital. We enrolled 180 consecutive patients diagnosed with thyroid nodules between January 2021 and December 2022. All participants underwent comprehensive ultrasound examinations comprising conventional US, CEUS, and UE. Fine-needle aspiration biopsy (FNAB) or surgical specimens were the gold standard for definitive diagnosis. Patients with inconclusive diagnoses or incomplete examinations were excluded. ***Results:*** Conventional US (ACR TI-RADS) achieved an AUC of 0.802, excelling in detecting suspicious features but suffering from inherent subjectivity. CEUS, with an AUC of 0.854 and a remarkable sensitivity of 95.29%, captured specific malignant patterns like centripetal enhancement and uneven distribution, but its reliance on contrast limited its applicability. UE provided an area under the curve (AUC) of 0.845 and valuable information about tissue stiffness, but its efficacy was influenced by nodule size and location. However, the true strength emerged when combining all three modalities. Multimodal ultrasound yielded an impressive AUC of 0.958 and a sensitivity of 91.76%, significantly surpassing individual performances. ***Conclusion:*** Our findings demonstrate that multimodal ultrasound, integrating conventional US, CEUS, and UE, significantly outperforms individual modalities in diagnosing thyroid nodules. Further research is warranted to refine and optimize this promising diagnostic strategy to benefit patients with thyroid nodules.

INTRODUCTION

The landscape of thyroid disease diagnosis has undergone a transformative shift in recent years, marked by a significant rise in the detection of thyroid nodules. This surge can be attributed to two key factors: the continued refinement of imaging technologies and the increasing prevalence of comprehensive screening programs [1]. For patients diagnosed with thyroid nodules, accurate differentiation between benign and malignant lesions becomes paramount, as appropriate management strategies directly impact their quality of life and long-term prognosis [2]. This, in turn, underscores the crucial role of a robust diagnostic approach capable of navigating the complexities of differentiating benign and malignant nodules [3].

Among various investigative tools, ultrasound has emerged as the preferred modality for thyroid nodule evaluation. Its accessibility, ease of operation, excellent reproducibility, and lack of ionizing radiation make it a desirable option [4]. Furthermore, conventional ultrasound provides detailed anatomical information regarding the nodule's location, size, shape, boundary, internal echo pattern, and calcifications, all vital elements in the initial assessment. However, despite its strengths, conventional ultrasound encounters limitations in definitively distinguishing benign from malignant nodules due to potential overlap in their ultrasonic features. This diagnostic challenge often necessitates reliance on the sonographer's clinical expertise and experience [5].

To overcome these limitations and enhance diagnostic accuracy, advanced ultrasound techniques like Contrast-Enhanced Ultrasound (CEUS) and Ultrasound Elastography (UE) have emerged as valuable adjuncts to conventional ultrasound (US) [6]. CEUS and ultrasound elastography UE technologies, which have rapidly advanced in recent years, complement conventional ultrasound examinations. They have found widespread use in the evaluation of thyroid nodule characteristics [7].

CEUS employs a low-mechanical-index approach and injects a contrast agent to visualize real-time microvascularization patterns within the nodule [8].

This dynamic visualization of blood flow aids in assessing vascularity, where specific patterns may raise suspicion for malignancy. In contrast, UE delves deeper into tissue properties by estimating tissue stiffness based on the structural composition of the extracellular matrix. This technique proves particularly valuable as pathological changes like tumors often exhibit increased tissue hardness, offering additional insights beyond conventional ultrasound findings [9].

This synergistic integration of conventional, contrast-enhanced, and elastography ultrasound truly unlocks the potential of "multimodal ultrasound." This innovative approach combines the strengths of each modality, leveraging their unique information streams to paint a more comprehensive picture of the thyroid nodule. By harnessing the detailed anatomy from conventional ultrasound, the vascular insights from CEUS, and the tissue characterization of UE, multimodal ultrasound strives to significantly improve diagnostic accuracy, specificity, and sensitivity in differentiating benign and malignant lesions [10].

This retrospective investigation meticulously explores the diagnostic effectiveness of multimodal ultrasound, focusing specifically on its ability to differentiate between benign and malignant thyroid nodules. Our analysis will encompass data from patients who underwent comprehensive examinations, incorporating conventional ultrasound, contrast-enhanced ultrasound (CEUS), and ultrasound elastography (UE). Subsequently, we will scrutinize and compare the acquired multimodal ultrasound findings with the well-established clinicopathological gold standard. Our study focuses on the novelty of incorporating comprehensive examinations, including conventional ultrasound, CEUS, and UE, in the evaluation of thyroid nodules. By comparing the multimodal ultrasound findings with the well-established clinicopathological gold standard, we seek to elucidate the true potential of multimodal ultrasound in enhancing the accuracy and confidence of thyroid nodule diagnosis.

PATIENTS AND METHODS

Patients

This retrospective study explores the diagnostic potential of multimodal ultrasound for differentiating benign and malignant thyroid nodules. Our data encompasses 180 patients (214 nodules) who underwent surgical or puncture pathology at Tangshan people's Hospital between 2021 and 2022. The patient population consisted of 96 males and 84 females, averaging 47.6 ± 7.6 years. Each participant underwent comprehensive examinations encompassing conventional ultrasound (US), contrast-enhanced ultrasound (CEUS), and ultrasound elastography (UE). To ensure the ethical conduct of the research,

the study protocol received formal approval from the Ethics Committee of the Tangshan people's Hospital (Approval Number: RMYY-LLKS-2025080 Date: June 19, 2025).

We carefully selected our study participants through stringent inclusion and exclusion criteria. To enhance the relevance and reliability of our findings, only patients who met specific requirements were included.

Firstly, patients had to have histologically con-firmed benign or malignant thyroid nodules through either surgical or puncture pathology. Additionally, participants were required to possess complete data from US, CEUS, and UE examinations. Participants meeting any of the following criteria were excluded from the analysis: Firstly, individuals with a history of prior thyroid surgery, including ablation, chemotherapy, radiotherapy, or other drug therapies, were excluded. Secondly, participants with known allergies to the contrast media used in CEUS examinations were also excluded. Furthermore, we excluded individuals with thyroid nodules located deep within the gland or obscured by thick neck muscle layers. These anatomical factors could potentially hinder the accuracy of the ultrasound assessment, making it challenging to obtain reliable results.

By employing this selection criteria, we aimed to minimize potential confounding factors and strengthen the validity of our conclusions regarding the diagnostic efficacy of multimodal ultrasound in distinguishing benign and malignant thyroid nodules.

Conventional ultrasound (US) inspection

We employed the GE LOGIQ E9 color Doppler diagnostic instrument (GE, USA) for all ultrasound examinations. The ML6-15 probe was used at a frequency range of 6-15 MHz for optimal image quality. Each participant maintained a supine position with their neck exposed during the examination. Our experienced sonographers explored both lobes and the isthmus of the thyroid gland, documenting critical features like:

Echo: The level of echoes reflected by the tissue was evaluated and categorized as none, high/equal, low, or very low.

Size: The dimensions of the thyroid gland and any identified nodules were measured.

Blood flow: The presence and pattern of blood flow within the thyroid gland and nodules were examined.

Additionally, nodule characteristics were also documented. These characteristics included the position of the nodule within the thyroid gland, its measured size, composition [cystic, spongy, mixed (cystic and solid components), or solid], echo: (internal echo level consistent with the categories used for the thyroid gland itself), shape (wider than tall or taller than wide), margin (smooth/unclear, irregular/lobulated, or close to the capsule/invading

the gland), and strong echo foci ((presence and distribution of calcifications or other punctate echoes, with categories including none, coarse, circular/marginal, or dot-like).

Two independent physicians employed the American College of Radiology Thyroid Imaging Reporting and Data System (ACR TI-RADS) scoring system to ensure standardized evaluation and minimize interobserver variability. In cases of disagreement, collaborative discussion and review ensured consensus on the final score. The ACR TI-RADS criteria are detailed below:

Internal Composition: Nodules that were cystic or almost cystic were given 0 points. Nodules classified as spongy were also assigned 0 points. Nodules that were cystic but had solid components received 1 point. Solid or almost solid nodules were given 2 points.

Echo Level: Nodules with no echo were assigned 0 points. Nodules with high or equal echo received 1 point. Nodules with low echo were given 2 points. Nodules with very low echo were assigned 3 points.

Shape: Nodules where the transverse diameter was greater than the anteroposterior diameter received 0 points. Nodules with an anteroposterior diameter equal to or greater than the transverse diameter were assigned 3 points.

Margin: Nodules with a smooth or unclear margin received 0 points. Nodules with an irregular or lobulated margin were assigned 2 points. Nodules with a margin that was close to the capsule or invading the gland received 3 points.

Strong Echo Foci: Nodules with no or large comet tail artifact were assigned 0 points. Nodules with coarse calcifications received 1 point. Nodules with a circular or marginal distribution of calcifications were given 2 points. Nodules with dot-like echoes were assigned 3 points.

The sum of individual scores across categories yielded the final ACR TI-RADS classification [11]: Nodules with a cumulative score of 0 points were classified as Class 1. Nodules with a cumulative score of 1 to 2 points were classified as Class 2. Nodules with a cumulative score of 3 points were classified as Class 3. Nodules with a cumulative score of 4 to 6 points were classified as Class 4. Nodules with a cumulative score of 7 points or more were classified as Class 5.

Contrast-enhanced ultrasound (CEUS) inspection

For CEUS examinations, we utilized a 9L probe operating at a frequency of 9 MHz. We identified the longitudinal section showcasing the target nodule's maximum long axis and adjusted the machine's settings to maintain moderate gain, depth, and focus for optimal image quality. Following standard procedures, we injected 1.5mL of Sonovue contrast agent (Bracco, Italy) via the cubital vein mass, immediately followed by 5mL of saline solution. This provided a clear window for observing the target nodule's dynamic enhancement patterns. We then continuously monitored the dynamic images for approximately 2 minutes and carefully selected an earlier frame with optimal contrast enhancement for further analysis.

Our assessment of CEUS findings focused on a range of qualitative parameters:

Enhancement direction: We described the pattern of contrast agent uptake within the nodule as either centrifugal (spreading outwards from the center) or centripetal (moving inwards from the periphery).

Enhancement intensity: This was visually compared to the surrounding normal thyroid tissue and categorized as low (less intense), equal, or high (more intense).

Contrast agent distribution: We described the spatial distribution of the contrast agent within the nodule as either uniform (evenly spread) or uneven (clumped or patchy).

Enhancement rate: We compared the speed of contrast agent uptake in the nodule relative to the surrounding normal thyroid tissue, classifying it as early progression (faster than normal), synchronous enhancement (matching normal tissue), or late progression (slower than normal).

Resolution speed: This captured the rate at which the contrast agent cleared from the nodule compared to the adjacent normal tissue, categorized as early regression (faster than normal), synchronous regression (matching normal tissue), or late regression (slower than normal).

Ultrasound elastography (UE) inspection

We employed the ML6-15 probe for UE examinations at a frequency range of 6-15 MHz. Unlike conventional ultrasound, UE mode requires positioning the probe perpendicular to the skin and applying gentle manual compression over the target lesion. This compression generates strain waves within the tissue, allowing us to assess its elasticity based on the degree of deformation.

The region of interest (ROI) encompassing the lesion was set at least twice its size to ensure accurate measurements. During the examination, we monitored the pressure gauge and promptly captured the image once the pressure reached level 3-4, providing optimal visualization of tissue response. To simplify interpretation, the elastography chart utilized a color-coded scheme:

Green: The color green represented the average hardness of tissues within the ROI, indicating normal elasticity.

Red: The color red was used to signify areas that were softer than the average. This could be indicative of fluid-filled structures such as cysts.

Blue: The color blue was used to indicate stiffer-than-average regions. This often correlated with denser or fibrotic tissues.

Based on the distribution of these color-coded areas within the ROI, we adopted a scoring system to categorize the lesion's elasticity:

Score 1: The lesion appeared green, implying normal tissue hardness throughout.

Score 2: Most of the lesion was green (at least 90% of the ROI), suggesting predominantly normal elasticity.

Score 3: The lesion displayed a roughly equal distribution of green and blue areas, hinting at a mixture of normal and stiffer-than-average tissues.

Score 4: The lesion was predominantly blue, either fully or with a minimal green component (over 90% of the ROI), indicating widespread increased tissue stiffness.

Our study's UE scores of 1-2 generally indicated benign lesions, as they reflected normal or predominantly normal tissue stiffness. Conversely, scores of 3-4 suggested a higher likelihood of malignancy due to the presence of stiffer-than-average areas, potentially associated with tumor growth or fibrosis. This interpretation aligns with established research suggesting a correlation between increased tissue stiffness and malignant characteristics in thyroid nodules.

Statistical analyses

The statistical analyses of the data were performed using SPSS 21.0 statistical software (SPSS Co., Ltd., Chicago, USA). The counting data were presented as frequencies or rates, and the Chi-square test was utilized for comparisons. To assess the diagnostic performance of each parameter in distinguishing between benign and malignant nodules, receiver operating characteristic (ROC) curves were constructed. Pathology results were used as the gold standard for comparison. The area under the curve (AUC) was calculated for each parameter. AUC > 0.70 indicated a statistical significance. $P < 0.05$ indicates a notable difference.

RESULTS

Pathological types of thyroid nodules

In this study, 180 patients were included, with 214 nodules in total (average diameter: (1.05±0.31) cm). The gold standard for determining the benign and malignant nodules was based on the pathological diagnosis obtained through either needle aspiration biopsy or surgical excision. The distribution of pathological types is presented in table 1.

Table 1. Pathological types of tumor amongst patients.

	Pathological type	Number of nodules	Proportion (%)
Benign (n = 129)	Nodular goiter	97	75.19
	Thyroiditis	25	19.38
	Adenoma	7	5.43
Malignant (n = 85)	Papillary carcinoma	78	91.76
	Medullary carcinoma	4	4.71
	Follicular cell carcinoma	2	2.35

ACR TI-RADS classification-based US results

The ACR TI-RADS classification-based evaluation of US and pathological results are compared in table 2. An ROC curve was generated based on the ACR TI-RADS classification-based evaluation results of US, yielding an AUC of 0.802, with sensitivity and specificity values determined to be 58.82% and 94.57%, respectively (figure 1).

Table 2. ACR TI-RADS classification-based US evaluation results.

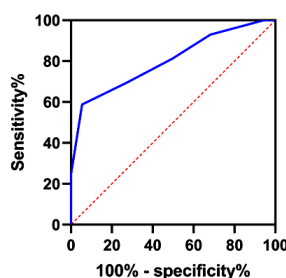|	Class 2	Class 3	Class 4	Class 5	Total
Benign	7	34	81	7	129
Malignant	0	6	29	50	85
Total	7	40	110	57	214

Note: ultrasound (US)

Figure 1. ROC curve of The ACR TI-RADS classification-based US diagnosis for thyroid nodules. An ROC curve illustrating the diagnostic performance of the American College of Radiology Thyroid Imaging Reporting and Data System (ACR TI-RADS) classification-based ultrasound (US) evaluation for thyroid nodules. The curve reveals an area under the curve (AUC) of 0.802. Sensitivity and specificity values, critical for evaluating the diagnostic accuracy, were calculated at 58.82% and 94.57%, respectively.

CEUS-based diagnosis of thyroid nodules

The pathological results were used as the reference standard to compare the CEUS findings of the thyroid nodules. The analysis revealed statistically significant differences between benign and malignant nodules in enhancement direction, enhancement level, contrast agent distribution, Enhancement rate and regression speed ($P < 0.05$). The indexes were assigned (table 3). The total score was calculated based on these indexes. ROC curve analysis was performed according to the gold standard of pathological results. It was found that the AUC was 0.854, and the sensitivity and specificity were 95.29% and 56.59%, as shown in figure 2.
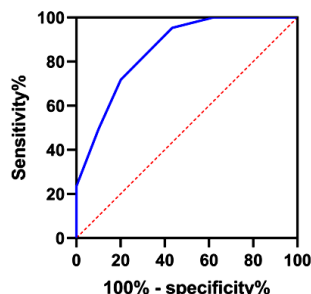
Figure 2. ROC curve of CEUS in diagnosing thyroid nodules. This figure illustrates the Receiver Operating Characteristic (ROC) curve of Contrast-Enhanced Ultrasound (CEUS) for diagnosing thyroid nodules. The analysis was conducted based on the gold standard of pathological results. The Area Under the Curve (AUC) was determined to be 0.854, with corresponding sensitivity and specificity values of 95.29% and 56.59%, respectively.

Table 3. Difference of CEUS characteristics in benign and malignant thyroid nodules.

Indexes		Benign (n=129)	Malignant (n=85)	c^2	P
Enhancement direction	Centrifugal	91 (70.54%)	21 (24.71%)	43.155	<0.001
	Centripetal	38 (29.46%)	64 (75.29%)		
Enhancement level	Low enhancement	50 (38.76%)	72 (84.71%)	44..558	<0.001
	Isoenhancement	44 (34.11%)	9 (10.59%)		
	High enhancement	35 (27.13%)	4 (4.71%)		
Contrast media distribution	Even	44 (34.11%)	8 (9.41%)	16.990	<0.001
	Uneven	85 (65.89%)	77 (90.59%)		
Enhancement rate	Early regression	36 (27.91%)	10 (11.76%)	21.611	<0.001
	Synchronous regression	48 (37.21%)	18 (21.18%)		
	Late regression	45 (34.88%)	57 (67.06%)		
Regression speed	Early regression	46 (35.66%)	46 (54.12%)	7.130	0.028
	Synchronous regression	44 (34.11%)	21 (24.71%)		
	Late regression	39 (30.23%)	18 (21.18%)		

Note: contrast-enhanced ultrasound (CEUS)

Table 4 outlines the scoring system for various Contrast-Enhanced Ultrasound (CEUS) characteristics in the evaluation of thyroid nodules. Scores are assigned based on enhancement direction, enhancement level, contrast media distribution, enhancement rate, and regression speed. The scoring system aims to standardize the interpretation of qualitative features observed during CEUS examinations, facilitating an objective and systematic analysis of thyroid nodules as part of multimodal ultrasound diagnosis.

Table 4. Assignment about CEUS characteristics.

Indexes		Score (point)
Enhancement direction	Centrifugal	0
	Centripetal	1
Enhancement level	Low enhancement	2
	Isoenhancement	1
	High enhancement	0
Contrast media distribution	Even	0
	Uneven	1
Enhancement rate	Early regression	0
	Synchronous regression	1
	Late regression	2
Regression speed	Early regression	2
	Synchronous regression	1
	Late regression	0

Note: contrast-enhanced ultrasound (CEUS)

UE-based diagnosis of thyroid nodules

The score results of UE for diagnosing thyroid nodules are presented in table 5. An ROC curve was generated based on the UE diagnosis results of the nodules, yielding an AUC of 0.845, with sensitivity and specificity values of 72.94% and 86.82%, respectively (figure 3).
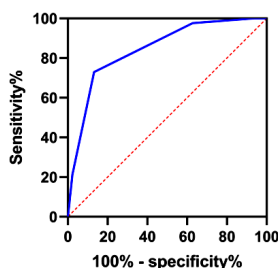

Figure 3. ROC curve of UE in diagnosing thyroid nodules. This figure presents the Receiver Operating Characteristic (ROC) curve, depicting the diagnostic performance of Ultrasound Elastography (UE) in discerning thyroid nodules. The generated ROC curve demonstrates an area under the curve (AUC) of 0.845. Sensitivity and specificity values crucial for evaluating diagnostic accuracy are reported at 72.94% and 86.82%, respectively.

Diagnostic efficacy evaluation of multimodal ultrasound for thyroid nodules

Binary Logistic regression analysis was performed on ACR TI-RADS classification-based US results, CEUS feature results, and UE diagnostic score results. These variables were used to construct a joint diagnostic model and diagnostic ROC curve was drawn. The results demonstrated that the combined diagnosis approach yielded an AUC of 0.958, with a sensitivity of 91.76% and a specificity of 86.05% (Figure 4). Comparing the diagnostic efficiency of different methods, it was evident that the AUC of the combined diagnosis was significantly higher than that of each individual diagnostic method.
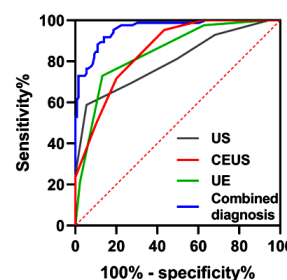

Figure 4. ROC curve of combined diagnosis and single diagnosis of thyroid nodules. The ROC curve represents the diagnostic performance of both the combined and single diagnostic approaches for thyroid nodules. Utilizing the variables, a joint diagnostic model was constructed, and the resulting ROC curve was analyzed. The combined diagnosis approach exhibited an impressive area under the curve (AUC) of 0.958. Sensitivity and specificity values, crucial for assessing diagnostic accuracy, were determined to be 91.76% and 86.05%, respectively.

Acquired ultrasound images

The images (figures 5-7) demonstrate the relevant and comprehensive visual representation of the nodular lesion in the left lobe of the thyroid gland, enabling clinicians to analyze its characteristics and aid in the diagnostic process.
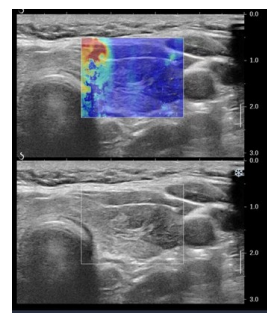

Figure 5. Conventional ultrasound and elastography images of the left lobe thyroid nodule.

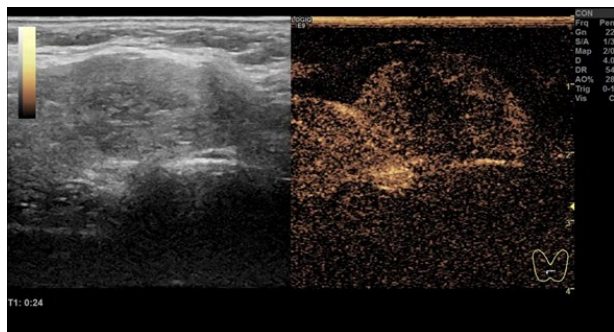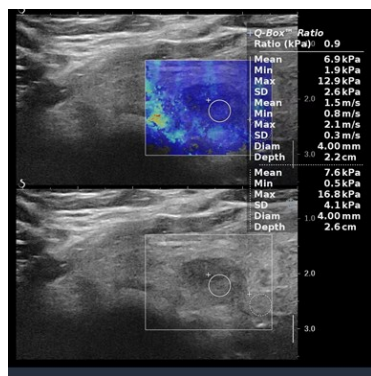**Figure 6.** Conventional ultrasound and elastography images of the left lobe thyroid nodule.

Figure 7. Ultrasound contrast imaging of the left lobe thyroid nodule.

DISCUSSION

High-resolution ultrasound probes are like microscopes for the thyroid gland, offering a detailed view of its nodules. They can reveal key features like tiny calcifications, dark patches (hypoechoic areas), irregular borders, stiffness, and even increased blood flow within the nodules – all clues potentially pointing towards malignancy [12]. Unfortunately, even with these detailed visuals, human interpretation comes into play, introducing variations in diagnosis depending on the individual physician's experience and skills [13].

This challenge has paved the way for multimodal ultrasound techniques like CEUS and UE, which combine real-time visualization with additional information about blood flow and tissue stiffness. Recent studies have shown promising results in improving diagnostic accuracy through this combined approach [14]. This is important because accurately distinguishing benign from malignant nodules is crucial in avoiding unnecessary surgeries and anxieties associated with overdiagnosis of low-risk cancers, while ensuring timely intervention for rarer aggressive tumors.

The ACR TI-RADS system acts like a standardized roadmap for interpreting ultrasound images. By systematically analyzing specific features of the nodules, it assigns a score corresponding to the likelihood of malignancy. Higher scores represent a higher risk [15]. In our study, we followed this roadmap to classify thyroid nodules after initial ultrasound examination. While the ROC curve

analysis showed a good AUC of 0.802, with decent sensitivity and specificity, it also highlighted the limitations of relying solely on ultrasound. There were still some misdiagnosed cases. This finding aligns with the work of Alyami *et al.*, who observed high consistency among Chinese doctors in assessing blood flow and calcifications, but significant inconsistencies in interpreting aspects like echo, shape, and edges [16].

In this study, Contrast-Enhanced Ultrasound (CEUS) emerges as a pivotal tool offering dynamic insights into the intricate blood flow patterns within and surrounding thyroid nodules [17]. By scrutinizing various CEUS indices, including enhancement direction, level, contrast agent distribution, enhancement rate, and regression speed, we discerned significant statistical disparities between benign and malignant nodules. The distinctive characteristics observed in malignant nodules, such as centripetal enhancement, low enhancement, uneven enhancement, late progression, and early regression, contribute to a nuanced understanding of their vascular dynamics. The observed low enhancement in malignant nodules can be attributed to diverse factors, including the presence of gravel calcification or varying degrees of interstitial tissue fibrosis within the nodules [18]. Furthermore, malignancies may manifest changes such as hemorrhage, necrosis, fibrosis, and calcification, giving rise to irregular contrast media distribution and uneven enhancement during angiography [19]. Notably, our findings align with existing literature, where neovascularization patterns in papillary thyroid carcinoma predominantly manifest in both peripheral and central regions. The density of neovascularization in the peripheral region typically exceeds that in the central region, resulting in an enhanced centripetal effect, wherein tumor-nourishing blood vessels flow from the periphery towards the center [20].

In our study, the Receiver Operating Characteristic (ROC) curve analysis underscores the diagnostic utility of CEUS, with an Area Under the Curve (AUC) of 0.854. This statistical measure, coupled with a sensitivity of 95.29% and specificity of 56.59%, highlights the discriminative prowess of CEUS in distinguishing between benign and malignant thyroid nodules. Our findings resonate with previous research by Zhao et al., emphasizing the efficacy of uneven enhancement observed in CEUS for diagnosing thyroid malignant nodules, particularly in cases concomitant with Hashimoto's thyroiditis [21]. Furthermore, our study extends this understanding, suggesting that CEUS enhances diagnostic accuracy in identifying thyroid nodules with an unknown malignant degree under conventional ultrasound (US).

Ultrasound Elastography (UE) serves as a valuable tool in our study, translating changes in

echo signal movement amplitude before and after compression into real-time color images. These images utilize an elastic encoding scheme to depict the stiffness or hardness of various tissues, providing a nuanced understanding of tissue characteristics. In normal tissues, where the differences in softness and hardness are relatively modest, this technique might have limited discriminative power. However, the pronounced variations in softness and hardness between normal and pathological tissues, with higher tissue elasticity coefficients in harder tissues, make UE particularly relevant for our investigation [22]. The observed tendency of malignant nodules to be harder than benign nodules align with the expected pathological characteristics. The nodular thyroid tissue, characterized by follicular formation and glial storage, exhibits a certain softness. In contrast, adenoma tissue, with a higher proportion of glial cells, manifests as a softer texture. The unique features of papillary carcinoma, where cancer cells grow in a papillary pattern surrounded by fibrous tissue and blood vessels, result in a sand-like appearance and a firm or hard texture [23]. This qualitative assessment through UE contributes valuable insights into the textural differences among thyroid nodules, enhancing our diagnostic capabilities.

Our study reveals that UE demonstrated an Area Under the Curve (AUC) of 0.845 in diagnosing thyroid nodules, achieving a sensitivity of 72.94% and specificity of 86.82%. Despite these promising results, it is crucial to acknowledge the inherent limitations of UE diagnosis. The anatomical intricacies of the neck can influence elastic imaging assessment, as variations in scan sections may impact the grading process. Furthermore, some criteria used in grading elasticity are relatively vague, leading to subjective interpretations and potential variability in diagnosis. These considerations underscore the importance of cautious interpretation when utilizing UE in clinical settings. Notably, our findings align with the research by Rago et al., highlighting that UE's diagnostic efficacy is not contingent on nodule size. High sensitivity and specificity were observed, even in nodules smaller than 1cm [24]. This robust performance across different nodule sizes enhances the clinical applicability of UE, suggesting its utility in detecting subtle variations in tissue elasticity across a spectrum of thyroid nodules. As we navigate the landscape of UE diagnostics, future research could further refine criteria for elasticity grading, ensuring standardized and reproducible results.

The culmination of our investigation employed a multi-modal ultrasound approach, strategically combining Ultrasonography (US), Contrast-Enhanced Ultrasound (CEUS), Ultrasound Elastography (UE), and additional indicators to enhance the differentiation between benign and malignant thyroid nodules. This comprehensive analytical framework allowed for a thorough evaluation of the ultrasonic characteristics inherent in these nodules. The sequential application of US served as an initial step to preliminarily discern the nature of the nodules. Subsequently, CEUS played a pivotal role in scrutinizing the distribution of blood vessels within the nodules, providing valuable insights into their vascular patterns. Additionally, the assessment of nodule hardness, a crucial determinant, was executed using Young's modulus obtained through Shear Wave Elastography (SWE). The amalgamation of these indices in a holistic manner facilitated a more accurate and nuanced evaluation of the nature of thyroid nodules.

The outcomes of our study underscore the efficacy of the multimodal ultrasound diagnosis, revealing an impressive Area Under the Curve (AUC) of 0.958. This AUC, notably higher than that achieved through single-diagnostic techniques such as US, CEUS, or UE in isolation, attests to the enhanced diagnostic capability of our comprehensive approach. The sensitivity and specificity of the multimodal strategy, standing at 91.76% and 86.05% respectively, further solidify its robust diagnostic performance, balancing both sensitivity and specificity effectively.

However, the application of Ultrasound Elastography (UE) in our study comes with inherent limitations that warrant careful consideration. Firstly, the unique anatomical structure of the neck introduces potential variability in elastic imaging assessment. The complex composition of muscles, vessels, and the thyroid itself can lead to variations in scan sections, impacting the grading process and potentially influencing the accuracy of UE diagnosis. The intricacies of neck anatomy demand cautious interpretation of UE results, especially given the dynamic nature of these structures. Additionally, the subjective nature of grading elasticity in UE poses a challenge to the reliability of results. While established criteria for grading exist, the application of these criteria may involve some degree of subjectivity. Different sonographers or clinicians may interpret nodule elasticity differently, leading to potential variations in diagnosis. Standardizing the criteria for elasticity grading becomes paramount to mitigate subjectivity and enhance the reproducibility of UE results. This need for standardization is crucial for the broader clinical adoption of UE. Furthermore, the sample data, predominantly comprising papillary thyroid carcinoma, limits the representation of other malignant nodule types, introducing potential biases in our outcomes. Additionally, the slightly broader inclusion range in the diameter of thyroid nodules warrants consideration in future studies, encouraging further stratification to explore potential impacts on diagnostic outcomes.

CONCLUSION

The integration of various ultrasound techniques under the umbrella of multimodal ultrasound provides a comprehensive and efficient evaluation of thyroid nodules' characteristics. This approach, marked by its heightened diagnostic accuracy, emerges as a valuable asset in the assessment of thyroid nodules, paving the way for improved diagnostic efficiency and, consequently, enhanced patient care. Future studies should explore the refining the stratification of nodule types and sizes to unravel more nuanced insights into the diagnostic potential of multimodal ultrasound.

REFERENCES

1. Offi C, Romano RM, Cangiano A, *et al*. (2021) Evaluation of LMR, NLR and PLR as predictors of malignancy in indeterminate thyroid nodules. *Acta Otorhinolaryngol Ital*, **41**(6): 530-6.
2. Alexander EK and Cibas ES (2022) Diagnosis of thyroid nodules. *Lancet Diabetes Endocrinol*, **10**(7): 533-9.
3. Antonia TD, Maria LI, Ancuta-Augustina GG (2023) Preoperative evaluation of thyroid nodules - Diagnosis and management strategies. *Pathol Res Pract*, **246**: 154516.
4. Durante C, Grani G, Lamartina L, *et al*. (2018) The diagnosis and management of thyroid nodules: A review. *JAMA*, **319**(9): 914-24.
5. Tessler FN, Middleton WD, Grant EG, *et al*. (2017) ACR thyroid imaging, reporting and data system (TI-RADS): White paper of the ACR TI-RADS Committee. *J Am Coll Radiol*, **14**(5): 587-95.
6. Chen H, Ye J, Song J, *et al*. (2021) Comparison of different ultrasound classification systems of thyroid nodules for identifying malignant potential: A cross-sectional study. *Clinics (Sao Paulo)*, **76**: e2126.
7. Xi X, Gao L, Wu Q, *et al*. (2020) Differentiation of thyroid nodules difficult to diagnose with contrast-enhanced ultrasonography and real-time elastography. *Front Oncol*, **10**: 112.
8. Radzina M, Ratniece M, Putrins DS, *et al*. (2021) Performance of Contrast-enhanced ultrasound in thyroid nodules: Review of current state and future perspectives. *Cancers (Basel)*, **13**(21): 5469.
9. Moraes PHM, Sigrist R, Takahashi MS, *et al*. (2019) Ultrasound elastography in the evaluation of thyroid nodules: evolution of a promising diagnostic tool for predicting the risk of malignancy. *Radiol Bras*, **52**(4): 247-53.
10. Han Z, Huang Y, Wang H, *et al*. (2022) Multimodal ultrasound imaging: A method to improve the accuracy of diagnosing thyroid TI-RADS 4 nodules. *J Clin Ultrasound*, **50**(9): 1345-52.
11. Hoang JK, Middleton WD, Tessler FN (2021) Update on ACR TI-RADS: Successes, challenges, and future directions, from the AJR special series on radiology reporting and data systems. *AJR Am J Roentgenol*, **216**(3): 570-8.
12. Tian Y, Lu Y, Zhao YZ, *et al*. (2018) Characteristics of high - resolution ultrasound in the assessment of microcalcification of papillary thyroid carcinoma. *Zhongguo Yi Xue Ke Xue Yuan Xue Bao*, **40**(3): 378-84.
13. Sun C, Zhang Y, Chang Q, *et al*. (2020) Evaluation of a deep learning -based computer-aided diagnosis system for distinguishing benign from malignant thyroid nodules in ultrasound images. *Med Phys*, **47**(9): 3952-60.
14. Valenciaga A, Ivancic RJ, Khawaja R, *et al*. (2021) Efficacy of an Integrated hands-on thyroid ultrasound session for medical student education. *Cureus*, **13**(1): e12421.
15. Xia R, Sun W, Yee J, *et al*. (2022) Do ACR TI-RADS scores demonstrate unique thyroid molecular profiles? *Ultrasonography*, **41**(3): 480-92.
16. Alyami J, Almutairi FF, Aldoassary S, *et al*. (2022) Interobserver variability in ultrasound assessment of thyroid nodules. *Medicine (Baltimore)*, **101**(41): e31106.
17. Wan P, Chen F, Liu C, *et al*. (2021) Hierarchical temporal attention network for thyroid nodule recognition using dynamic CEUS imaging. *IEEE Trans Med Imaging*, **40**(6): 1646-60.
18. Kogai T, Taki K, Brent GA (2006) Enhancement of sodium/iodide symporter expression in thyroid and breast cancer. *Endocr Relat Cancer*, **13**(3): 797-826.
19. Kurti M, Sabeti S, Robinson KA, *et al*. (2023) Quantitative biomarkers derived from a novel contrast-free ultrasound high-definition microvessel imaging for distinguishing thyroid nodules. *Cancers (Basel)*, **15**(6): 1888.
20. Skuletic V, Radosavljevic GD, Pantic J, *et al*. (2017) Angiogenic and lymphangiogenic profiles in histological variants of papillary thyroid carcinoma. *Pol Arch Intern Med*, **127**(6): 429-37.
21. Zhao RN, Zhang B, Yang X, *et al*. (2015) Diagnostic value of contrast -enhanced ultrasound of thyroid nodules coexisting with Hashimoto's thyroiditis. *Zhongguo Yi Xue Ke Xue Yuan Xue Bao*, **37**(1): 66-70.
22. Liu T, Ge X, Yu J, *et al*. (2015) Comparison of the application of B-mode and strain elastography ultrasound in the estimation of lymph node metastasis of papillary thyroid carcinoma based on a radiomics approach. *Int J Comput Assist Radiol Surg*, **13**(10): 1617-27.
23. Moon HJ, Kim EK, Yoon JH, *et al*. (2012) Clinical implication of elastography as a prognostic factor of papillary thyroid microcarcinoma. *Ann Surg Oncol*, **19**(7): 2279-87.
24. Rago T, Vitti P. (2009) Potential value of elastosonography in the diagnosis of malignancy in thyroid nodules. *Q J Nucl Med Mol Imaging*, **53**(5): 455-64.